

Faraday Discussions

Accepted Manuscript



This is an Accepted Manuscript, which has been through the Royal Society of Chemistry peer review process and has been accepted for publication.

Accepted Manuscripts are published online shortly after acceptance, before technical editing, formatting and proof reading. Using this free service, authors can make their results available to the community, in citable form, before we publish the edited article. We will replace this Accepted Manuscript with the edited and formatted Advance Article as soon as it is available.

You can find more information about Accepted Manuscripts in the [Information for Authors](#).

Please note that technical editing may introduce minor changes to the text and/or graphics, which may alter content. The journal's standard [Terms & Conditions](#) and the [Ethical guidelines](#) still apply. In no event shall the Royal Society of Chemistry be held responsible for any errors or omissions in this Accepted Manuscript or any consequences arising from the use of any information it contains.

This article can be cited before page numbers have been issued, to do this please use: E. Gyasi Agyemang, S. Confederat, G. Mohanan, M. A. Sani, C. Chau, D. Charnock, C. Walti, K. Tschulik, M. Edwards and P. Actis, *Faraday Discuss.*, 2024, DOI: 10.1039/D4FD00143E.

Multimodal nanoparticle analysis

View Article Online
DOI: 10.1039/D4FD00143E

enabled by a polymer electrolyte nanopore combined with nanoimpact electrochemistry

Eugene Gyasi Agyemang^{1,#}, Samuel Confederat^{2,3,#}, Gayathri Mohanan^{2,3,#}, Manhaz
Azimzadeh Sani⁴, Chalmers Chau^{2,3}, Dylan Charnock^{2,3}, Christoph Wälti^{2,3}, Kristina
Tschulik⁴, Martin Andrew Edwards^{1,*}, Paolo Actis^{2,3*}

¹ Department of Chemistry and Biochemistry, University of Arkansas, Fayetteville, AR,
72701, USA

² Bragg Centre for Materials Research, University of Leeds, LS2 9JT, UK

³ School of Electronic and Electrical Engineering and Pollard Institute, University of Leeds,
Leeds LS2 9JT, UK

⁴ Ruhr University Bochum, Universitätsstraße 150, 44801 Bochum, Germany

These authors contributed equally to the work

* Corresponding authors; maedw@uark.edu; p.actis@leeds.ac.uk



ABSTRACT

View Article Online
DOI: 10.1039/D4FD00143E

Nanopores are emerging as a powerful tool for the analysis and characterization of nanoparticles at the single entity level. Here, we report that a polymer electrolyte nanopore system enables the enhanced detection of nanoparticle at low ionic strength when a PEG-based polymer electrolyte is present inside the nanopore.

We developed a numerical model that recapitulates the electrical response of the nanopore system and the model revealed that the electrical response of the glass nanopore is sensitive to the position of the polymer electrolyte interface.

As proof of concept, we demonstrated the multimodal analysis of a nanoparticle sample by coupling the polymer electrolyte nanopore sensor with nanoimpact electrochemistry. This combination of techniques could deliver the multiparametric analysis of nanoparticle systems complementing electrochemical reactivity data provided by nanoimpact electrochemistry with information on size, shape and surface charge provided by nanopore measurements.



INTRODUCTION

Over the past decades, nanoparticles have played significant roles in scientific and technological disciplines, ranging from medicine to materials science.^{1,2} Characterizing functional nanoparticles' physical parameters (size, shape, etc.) coupled with chemical reactivity is crucial for determining structure–function relationships and to guide future developments.³ Moreover, the ability to characterize nanoparticles in solution and in real-time is of utmost importance as it would allow, for example, in-flow optimization of nanoparticle synthesis or characterization of dynamic processes in solution.⁴ However, physico-chemical characterization of nanoparticles in heterogenous mixtures is challenging.⁵ While dynamic light scattering (DLS) or UV-Vis spectroscopy provide robust information on size distributions, they are ensemble-averaging techniques and, therefore, fall short in fully characterizing heterogenous nanoparticle mixtures.⁶ Nanoparticle tracking analysis (NTA) can analyse polydisperse nanoparticles with single-entity resolution, however the nanoparticles need to have a refractive index distinct from the surrounding medium or be modified with a fluorescent label.⁷ Electron microscopy approaches such as transmission electron microscopy (TEM) provide high-resolution characterization of individual nanoparticles but suffer from sampling bias, low throughput, and require careful sample preparation and are ex situ.³

Nanopore sensing, shown schematically in Figure 1, is a powerful label-free electrical technique where single entities passing through a small opening between two electrolyte-filled electrode-containing reservoir cause a temporary current modulation. In the figure, as in this work, the interior of a nanopipette is one reservoir while the orifice at the end the



pipette is the nanopore. The magnitude, duration and shape of the current modulation

reflect the physical properties ⁸ (*e.g.*, size, shape, charge) of the analyte and its translocation

dynamics as it is driven through the pore by an electric field and/or other forces ⁹. We have shown the large enhancement of the detection sensitivity of a conical glass nanopore with the addition of the polymer polyethylene glycol (PEG) to the electrolyte in the external bath solution.^{10, 11} This discovery enabled the probing of viral RNAs,¹⁰ the supramolecular assembly of DNA origami, ¹² and the high-throughput characterization of heterogeneous nanoparticle mixtures at low ionic strength.¹³

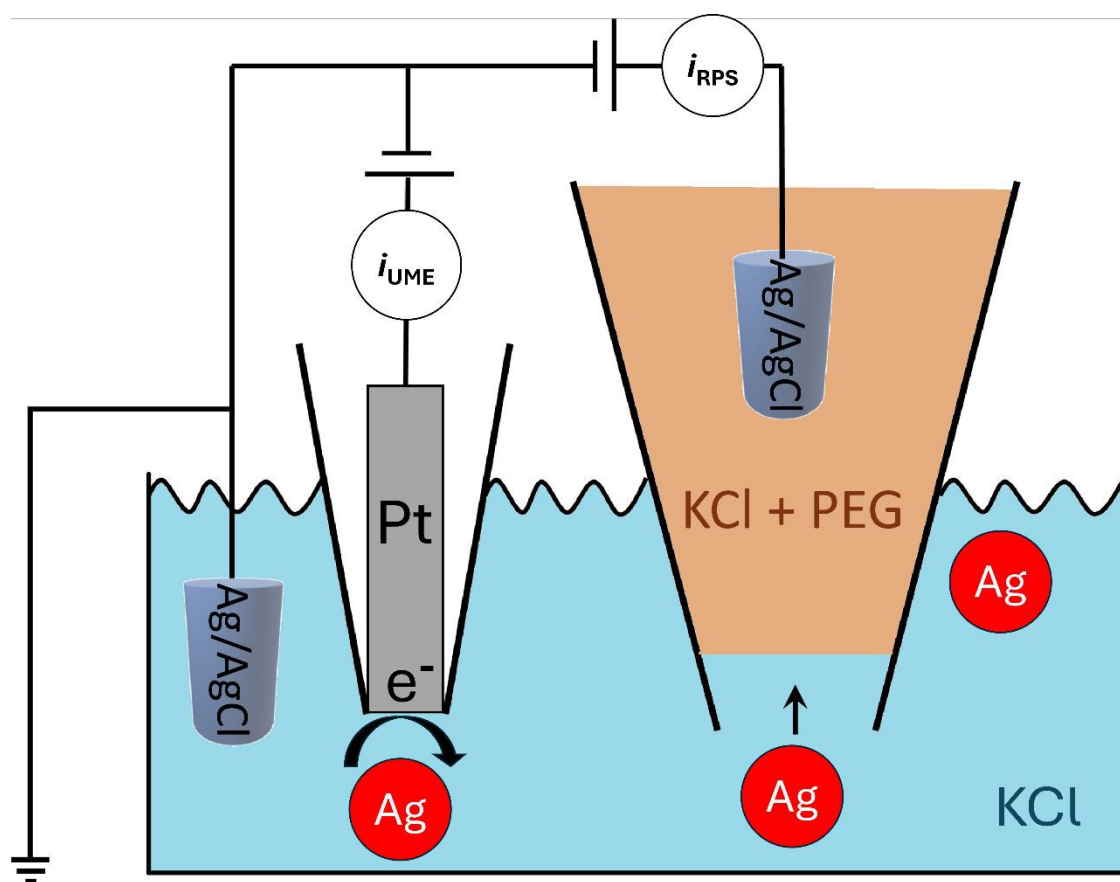


Figure 1. Schematic of experimental setup for nanopore sensing and nanoimpact electrochemistry.

Our interpretation of the mechanism of enhancement is based on evidence that the affinity of cations to PEG causes a higher anion transference number in PEG compared to aqueous



solutions, which generates a voltage-dependent ion concentration at the nanopore opening.

[View Article Online](#)

[DOI: 10.1039/D4FD00143E](https://doi.org/10.1039/D4FD00143E)

This results in ion enrichment at positive potentials and ion depletion at negative potentials

(measured as the internal electrode vs. ground in the bath). Furthermore, we postulated the

interface near the nanopore opening that gets disrupted but the translocation of an analyte.

We demonstrated using a range of model analytes that such interactions could lead to

alteration of the ion distribution at the tip orifice, which can result in temporary current

increases.^{10-12, 14}

Our mechanistic description of the system suggests that ion transport in and around the

interface between the polymer electrolyte and the aqueous solution plays a key role in

determining the sensitivity of the system. Herein, we investigate the reverse approach when

the polymer electrolyte is placed inside the pipette and the nanoparticle samples in the

bath, a format more amenable to sensing applications.

We report that the signal enhancement is also obtained when the nanoparticle translocations

are performed in a bath-to-nanopore configuration and the polymer electrolyte only present

in the nanopore, as shown in Figure 1. We developed a numerical model that recapitulates

the electrical response of the nanopore system and provides a physical explanation for the

enhanced current. Furthermore, we show the multimodal analysis of a nanoparticle sample

by coupling nanopore sensing with nanoimpact electrochemistry. Nanoimpact

electrochemistry allows the high throughput electrochemical analyses of colloidal (sub-

)micro- to nanometer sized particles based on their stochastic collisions on a micro- or

nano-electrode.¹⁵ This combination of techniques could allow for the multiparametric analysis

of nanoparticle systems where the information on size, shape and surface charge provided



by nanopore sensing can be merged with the (electro)chemical reactivity data provided by nanoimpact electrochemistry.

View Article Online
DOI: 10.1039/D4FD00143E

RESULTS AND DISCUSSION

Electrochemical Characterization

We demonstrated that a polymer electrolyte nanopore system enables the enhanced detection of nanoparticle samples when a PEG-based polymer electrolyte is present inside the nanopipette.

We first developed a numerical model was developed that allows determination of the coupled electric potential and ion transport within the system. The model, which is described in detail in the Supporting Information (Figure S1), is based on that described in Marcuccio et al.¹⁴ Briefly, the nanopipette is described as a truncated cone with charged glass walls that are impermeable to ions. The bulk concentration of the ions is fixed far inside the pipette and far into the bath solution at the experimentally prepared concentration (20 mM KCl) while a potential bias, E , is applied between an electrode inside the pipette vs. ground in the bath solution. The current is calculated by integrating the fluxes of both ions across the internal electrode (eq. S3).

The transport properties of the ions in the aqueous and PEG-containing phases, the geometry of the pipette, and the surface charge on the glass were all calculated from complementary experimental measurements, as detailed in Supporting Information section S2 (Figure S2, S3). As can be seen in Figure 2, simulations using these parameters (solid lines) quantitatively match experiments (points) both when the nanopipette contains 20



mM KCl (black; no PEG) or 20 mM KCl + 25% (w/v) 35K PEG (orange; PEG) that is immersed in a bath containing 20 mM KCl (Figure S4).

View Article Online
DOI: 10.1039/D4FD00143E

While the interface between the PEG-containing and aqueous electrolytes likely occupies a finite width mixing region, to avoid adding additional parameters to the model, we describe it as a discrete interface (see inset to Figure 2). When the interface is modelled as residing exactly at the pipette orifice, poor agreement is observed between the experimental and simulated i - E response (see Supporting Information section S3, Figure S6). Yet when the interface is moved slightly inside the pipette ($Z_{\text{int}} = 8 \mu\text{m}$), as can be seen in Figure 2, the simulated current (orange line) quantitatively captures the experimental voltammetric behavior (orange points). This apparent position of the interface likely accounts for the finite width of the interface and possibly how easily the viscous PEG-containing solution enters the nanopipette when backfilled.

The voltammetric response of a 20 mM PEG-electrolyte filled nanopipette immersed in a bath containing 20 mM KCl is nonlinear (rectified), with lower current magnitudes at positive potentials compared to their negative counterparts. At all potentials, the currents for the PEG-containing pipette (orange) are lower than their counterparts for the no-PEG case (black). The rectification can be understood by consideration of the ion distributions within the pipette at representative potentials of ± 0.5 V, which are shown in Figure 3 (see Supporting Information for concentrations at other potentials). Note, for simplicity Figure 3 showed the average ion concentration, however this is representative of the K^+ and Cl^- concentration in all but the electric double layer (see Supporting Information for details). At negative potentials, red and orange colors indicate the concentration just inside the nanopipette is higher than the bulk concentration (blue-green color; 20 mM), whereas at



positive potentials the concentration is diminished (dark blue). These swings in concentration cause the corresponding changes in resistance that cause the rectified $i-E$ response for the PEG-electrolyte filled nanopipette.

View Article Online

DOI: 10.1039/D4FD00143E

A quantitative comparison can easily be achieved by considering the axial concentration distribution along the pipette, which is shown in the lower part of Figure 3. The solid lines, which are from taken with the same conditions as the upper panel (PEG in pipette/KCl bath), but over a greater vertical range show the concentration is enhanced up to 32% (-0.5 V) or decrease by as much as 25% (+0.5 V), with each extremum occurring at the location of the PEG/KCl interface ($z = 8 \mu\text{m}$). The dashed lines show the changes in concentration with no PEG in the pipette, which are due to the surface charge and geometric asymmetry of the conical nanopore.¹⁶ They are much smaller ($\pm 2\%$) relative to the PEG-in-pore configuration, but with the enhancement and depletion again occurring at negative and positive potentials, respectively (see Supporting Information for colour plots for this condition). The small potential-dependent concentration variation, and hence change in conductivity, for the KCl/KCl case explains why the $i-E$ response (black line Figure 2) is close to linear. Interestingly, while the concentration inside PEG-electrolyte containing nanopipette at -0.5 V is greater than at the same potential for a non-PEG containing electrolyte the diminished mobilities in PEG lead to an overall lower current.

To understand the origin of the ion accumulation/depletion with the PEG-electrolyte containing nanopipette requires consideration of the transport of the two ions in both phases. While the increased viscosity of the PEG solution leads to lower conductivity (0.119 S/m vs 0.386 S/m in 20 mM KCl) there are differences in the relative values of the diffusion coefficients (Figure S5). While the transference numbers of K^+ and Cl^- in aqueous electrolyte



are approximately equal ($D_{K^+}/D_{Cl^-} \approx 0.96$)¹⁷ the affinity of cations for the PEG leads to K^+ having a lower transference number than Cl^- with $D_{K^+}^{PEG}/D_{Cl^-}^{PEG} \approx 0.82$. This leads the interface between the PEG-containing and aqueous electrolytes to behave selectively for the transport of anions. At negative potentials, the anion-selective nature of the interface leads the cations that are driven inwards by the electric field to accumulate near the interface. This in turn triggers a compensatory accumulation of anions to maintain electroneutrality. At positive potentials, the opposite is true and the concentration around the end of the pipette decreases.

Ion current rectification in nanopores is typically associated with the charge on the glass surface introducing ion selectivity to a nanopore when the double layer thickness is a significant proportion of the pore diameter.^{16, 18} Yet in the PEG-electrolyte system the ion selectivity arises from a fundamentally different mechanism. This can be confirmed by simulations in which the surface charge is set to 0 and which show negligible change in the rectified i - E response (see Supporting Information section S4, Figure S7-S11).

View Article Online

DOI: 10.1039/D4FD00143E



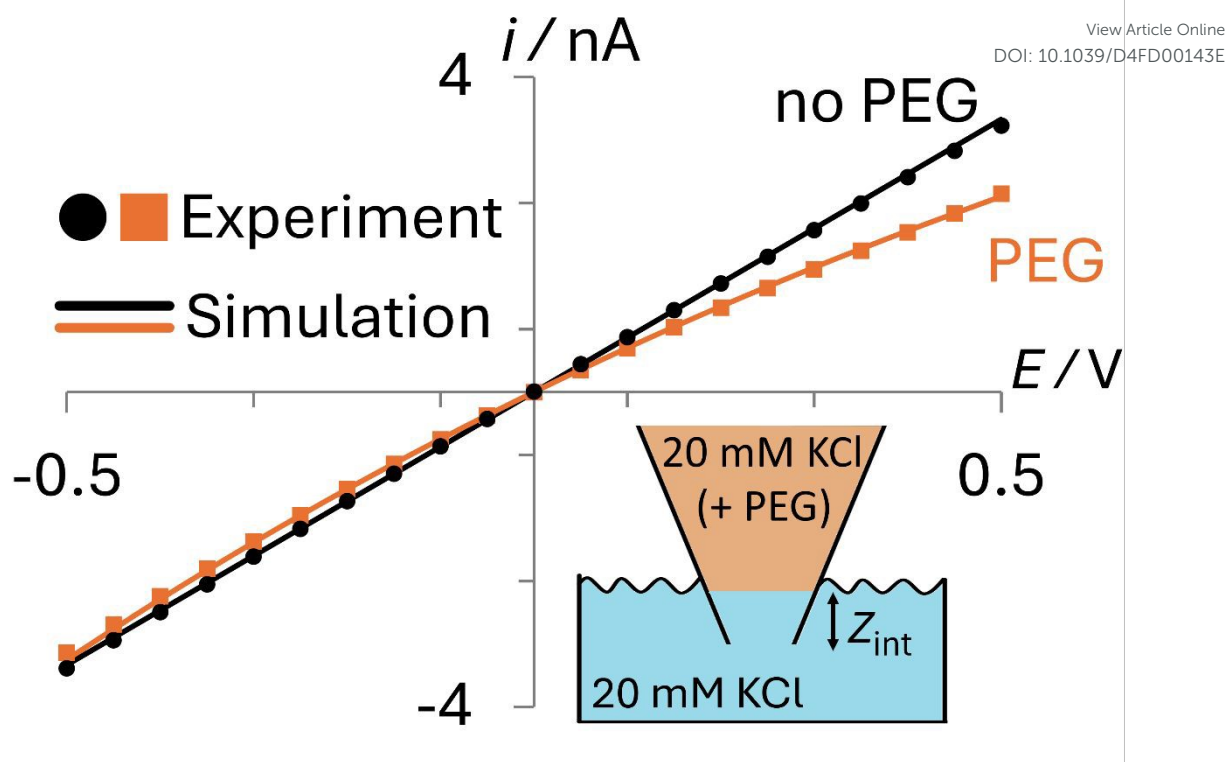


Figure 2. Comparison of experimental (points) and simulated (lines) i - E responses for PEG-containing (orange) and no PEG (black) electrolyte filled 70-nm radius nanopipettes. Bath solution: 20 mM KCl (no PEG). Pipette fill solution: 20 mM KCl with 25% (w/v) 35K-PEG. Interface between phases at $z_{int} = 8 \mu\text{m}$.



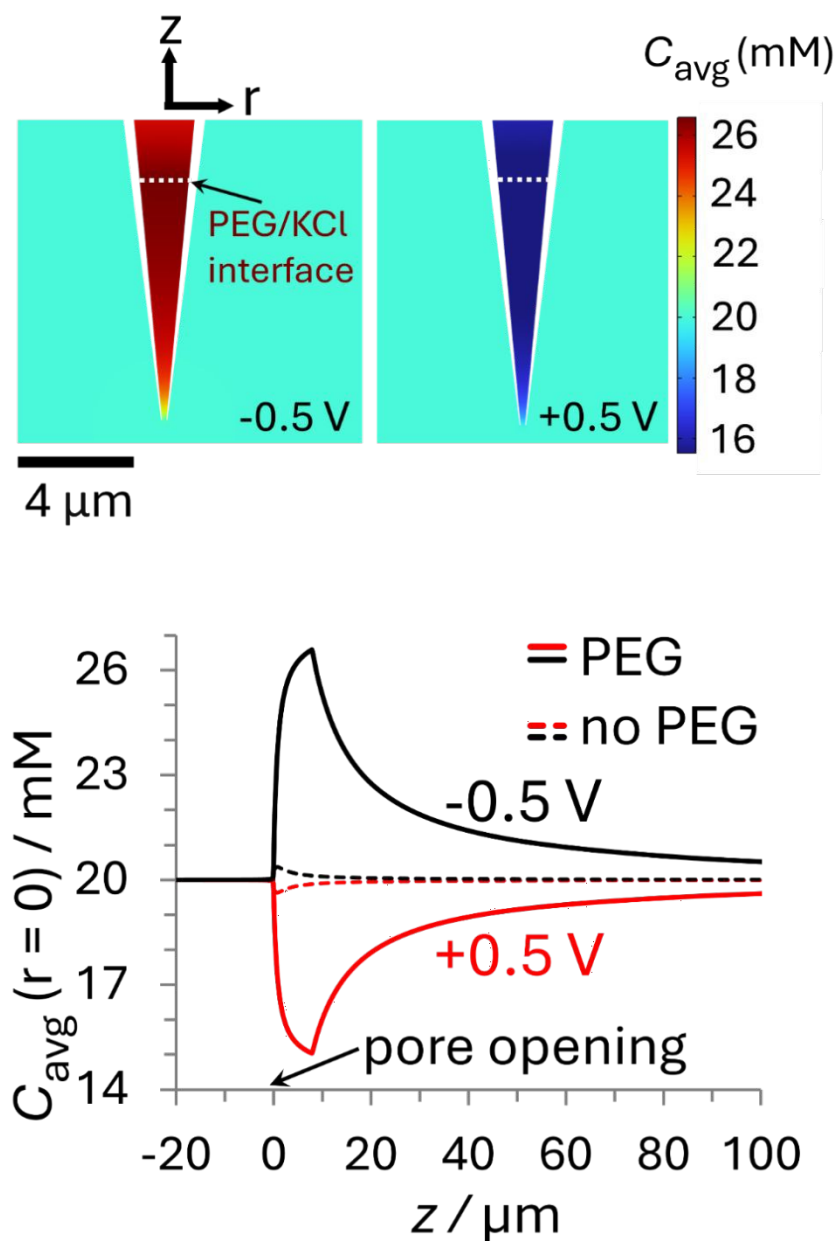


Figure 3 Plots of the simulated ion concentration around the nanopipette tip at ± 0.5 V. (top) Color plots of average concentration ($C_{\text{avg}} = 1/2([K^+] + [Cl^-])$) for the PEG-in-nanopipette / KCl-in-bath configuration at (left) -0.5 V and (right) $+0.5$ V. White dashed line represents interface between phases at $z_{\text{int}} = 8 \mu\text{m}$. (bottom) Average ion concentrations along the nanopipette axis of symmetry. The solid curves are for the PEG-in-Nanopipette / KCl-in-Bath configuration and the dashed lines for KCl in the bath and nanopipette (no PEG). Nanopipette radius: 70 nm . PEG: 25% (w/v) PEG 35K + 20mM KCl. KCl: 20mM KCl. The individual cation and anion concentration distributions are included in the Supporting Information. For color plots of C_{avg} with 20 mM KCl in the bath and nanopipette see Supporting Information. See Supporting Information for axial concentrations at other potentials.



Nanoparticle Translocations

View Article Online

DOI: 10.1039/D4FD00143E

A glass nanopore filled with a polymer electrolyte enables the enhanced detection of nanoparticles. We first fabricated a glass nanopore of 140 nm in diameter (matching the one used in the simulations above) and we only observed signal nanoparticle translocations when the nanopore was filled with a solution of 25% 35K PEG + 20 mM KCl (Fig S12) and immersed in an electrolyte (KCl) solution where the application of a potential between a pair of Ag/AgCl electrodes, inside the glass nanopore and external bath drives the translocation of the nanoparticle from the trans chamber (bath) to the cis chamber (inside the glass nanopore). To improve the signal to noise ratio, we then fabricated glass nanopores with a diameter of 60 nm and probed the translocation of 30-nm diameter silver nanosphere under a range of applied voltages (Figure 4). The nanopore setup consisted of a glass nanopore filled with a solution of 25% 35K PEG + 20 mM KCl and immersed in an electrolyte (KCl) solution where the application of a potential between a pair of Ag/AgCl electrodes, inside the glass nanopore and external bath drives the translocation of the nanoparticle from the trans chamber to the cis chamber. Figure 4 shows a representative ion current traces with increasing applied voltage where individual nanoparticle translocations can be identified from 200mV.



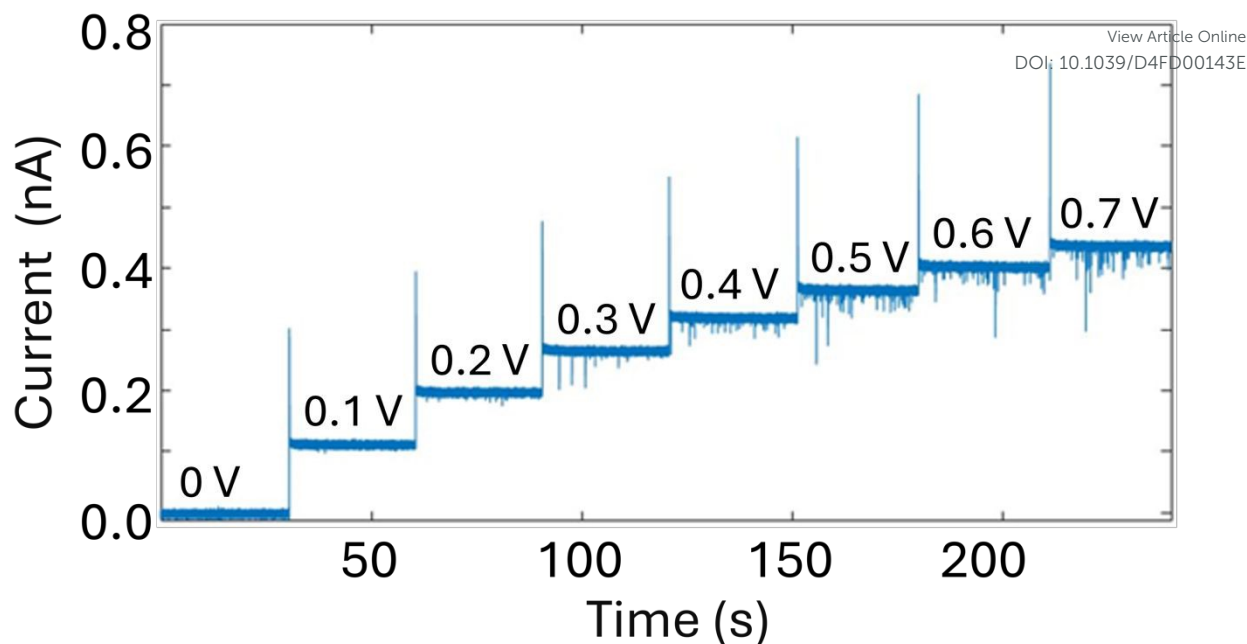


Figure 4. Nanopore measurements of a solution of 0.04 mg/mL 30-nm-diameter citrate Ag NPs dissolved in 20 mM KCl using a 60-nm diameter glass nanopore filled with 25% PEG 35K and 20 mM KCl with increasing applied potential. Reference electrode: Ag/AgCl frit filled with 20 mM KCl. Measurements performed with the Elements srl Nanopore reader at a sampling frequency of 100 kHz.

Interestingly, the presence of the polymer electrolyte inside the glass nanopore enhances both the amplitude and the number of the translocation events thus facilitating nanoparticle detection (Figure 5). We observed a similar enhancement when the polymer electrolyte was only present in the bath solution but it has to be noted that in the “nanopore-to-bath” configuration the nanoparticle translocation lead to conductive events while in the “bath-to-nanopore” we observed only resistive events. This indicates that the mechanism responsible for the signal enhancement could be different that the one reported before¹⁴ and its precise elucidation will require further work which is beyond the scope of this paper.



Also, nanoparticles translocations can be observed also under very low ionic strength solution (5mM KCl) and we have also demonstrated the detection of Pt nanoparticle translocation directly in a citrate buffer without the addition of any supporting electrolyte (Figure S13). The amplitude of the single entity events decreases with decreasing concentrations of the supporting electrolyte but, even in absence of KCl, the signal to noise ratio is large enough to allow the robust identification of single entity events.

View Article Online

DOI: 10.1039/D4FD00143E

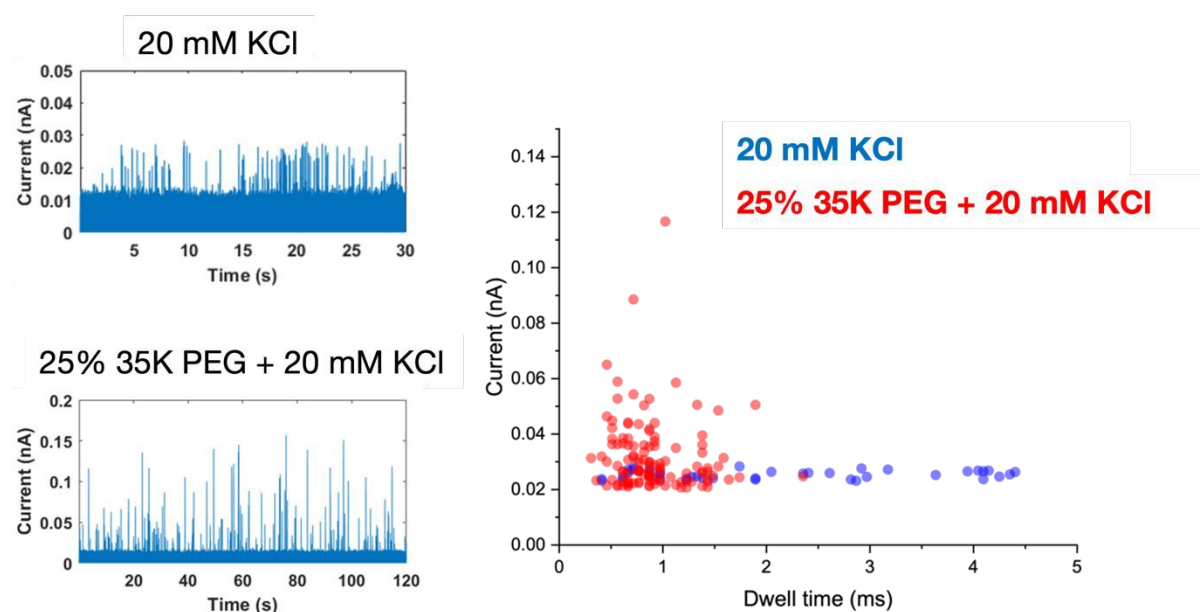


Figure 5. Nanopore measurements of a solution of 0.04 mg/mL 30-nm-diameter citrate-capped Ag NPs dissolved in 20 mM KCl using a 60-nm-diameter glass nanopore a) either filled 20 mM KCl or with 25% PEG 35K and 20 mM KCl. b) Scatter plots of the single nanoparticle translocation events with a glass nanopore filled with 20 mM KCl (blue dots) or 25% PEG 35K and 20 mM KCl (red dots). Reference electrode: Ag/AgCl frit filled with 20 mM KCl. Measurements performed with the Elements srl Nanopore reader at a sampling frequency of 100 kHz. Applied potential 700 mV.

An important consequence of enabling outside-to-in nanoparticle analysis is that multiple sensors can be integrated in the trans chamber to enable multimodal nanoparticle detection. As a proof-of-concept, we demonstrate the integration of a Pt-microelectrode within the trans chamber to perform nanoimpact measurements of the Ag nanoparticle



sample. Nanoimpact experiments rely on random collision of micro or nanoparticles with a polarized electrode due to their Brownian motion in solutions, thus providing an efficient approach for electrochemical detection and characterization of electrochemically active nanoparticles. Oxidative nanoimpact events can be detected from an applied voltage of 100 mV (vs Ag/AgCl) and their amplitude increases with increasing applied voltages (Figure 6) demonstrating the experimental setup and the buffer environment is compatible for a multi-sensor analysis of nanoparticle samples.

View Article Online

DOI: 10.1039/D4FD00143E

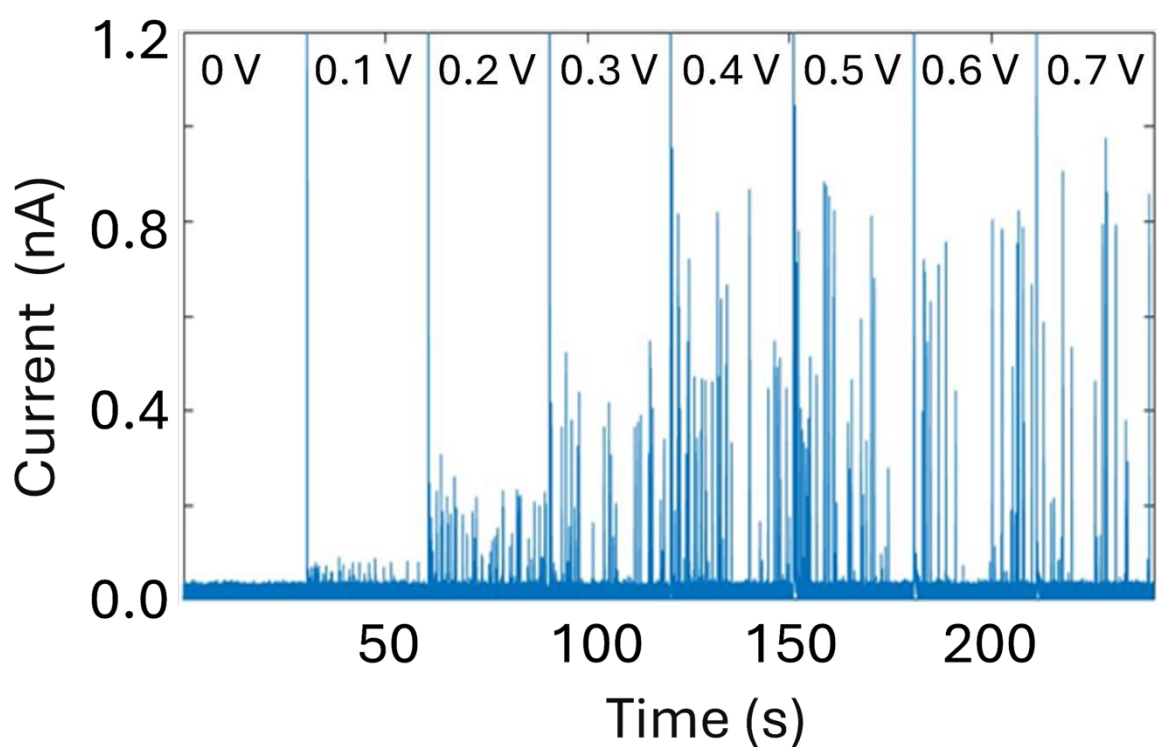


Figure 6. Nanoimpact measurements of a solution of 0.04 mg/mL 30 nm citrate Ag NPs dissolved in 20 mM KCl using a Pt ultramicroelectrode (10 μm in diameter) with increasing applied potential. Reference electrode: Ag/AgCl frit filled with 20 mM KCl. Measurements performed with the Elements srl Nanopore reader at a sampling frequency of 100 kHz.



DISCUSSION

View Article Online
DOI: 10.1039/D4FD00143E

Here we reported the combination of nanopore sensing with nanoimpact electrochemistry to provide enhanced analysis of nanoparticle samples. This approach combines size, charge and volume sensitivity of nanopore sensing with the ability of nanoimpact electrochemistry to probe electrochemical activity. This approach uniquely enables the detection of nanoparticles under low ionic strength (20mM) which is still a great challenge in nanopores sensing, potentially allowing the detection of a nanoparticle samples prone to aggregation under high ionic strength. In future, also sensor fusion approaches¹⁹ can be integrated to combine the outputs of both sensors to provide precise physical and chemical characterization of heterogenous nanoparticles samples. Importantly this integration will also require advancements in the signal processing algorithms to take full advantages of advanced machine learning routines²⁰⁻²².

The approach described in this work involves two distinct sensors (a glass nanopore and a Pt microelectrode) to perform the multimodal nanoparticle analysis but Pandey et al have shown that an integrated nanopore-nanoelectrode setup can be implemented for single entity detection²³ and for intracellular delivery²⁴. Similarly, Ren et al constructed a nanopore field-effect transistor that could also be employed for multimodal nanoparticle sensing²⁵. An alternative approach could also rely on the application of pressure to drive the nanoparticle translocations²⁶.

Also this work complements the work by Kawaguchi et al²⁷ that reported the enhanced nanoparticle sensing in a highly viscous nanopore by showing that also the interfacial properties at the nanopore are responsible for its sensing performance.



The key advantage of utilising nanopipettes is that they can be integrated with micromanipulators and multi-well plates, in an a similar ay to liquid handling robots, to enable the automated analysis of several analytes sequentially in a similar way to the work of Liang *et al* where they employed a robotic electrochemical reader for biosensing²⁸. Also, nanopipettes can be integrated with nanomanipulators to comprise a scanning probe microscopy setup to allow for the nanoscale analysis of single entities²⁹.

View Article Online

DOI: 10.1039/D4FD00143E

CONCLUSION

We have shown that there is a significant enhancement of the detection sensitivity of a conical glass nanopore, for bath-to-nanopore translocating events, when the nanopore electrolyte is composed of 25% (w/v) 35K-PEG in 20 mM KCl.

We developed a numerical model that recapitulates the electrical response of the nanopore system and provides a physical explanation for the enhanced current. Our interpretation of the mechanism of enhancement is based on evidence that the affinity of cations to PEG causes a higher anion transference number in PEG compared to aqueous solutions, which generates a voltage-dependent ion concentration distribution in the vicinity of the nanopore orifice with a concentration enhancement at negative biases and depletion at positive biases. The model reveals that the electrical response of the glass nanopore is sensitive to the position of the PEG interface.

As proof of concept, multimodal analysis of a nanoparticle sample was demonstrated by coupling the polymer electrolyte nanopore sensor with nanoimpact electrochemistry. This combination of techniques could deliver the multiparametric analysis of nanoparticle systems



yielding (electro)chemical reactivity data provided by nanoimpact electrochemistry in addition to information on size, shape and surface charge provided by nanopore measurements. We hope that this approach will lead to new insights in structure-function relationships of functional nanoparticles.

[View Article Online](#)

DOI: 10.1039/D4FD00143E



MATERIALS AND METHODS

View Article Online
DOI: 10.1039/D4FD00143E

Chemicals and materials

All reagents used in the translocation experiments were prepared using ultra-pure water (18.2 M Ω .cm) from Millipore system and further filtered through a 0.22 μ m syringe. KCl, Triton-X, EDTA, and PEG reagents were purchased from Sigma Aldrich. Ag and Pt spherical nanoparticles (citrate capped, 30 nm radius) were purchased from the nanoXact range from Nanocompositix and were used as received. Silver wire (0.25 mm diameter) used in the nanopore experiments were obtained from Alfa Aesar.

Electrolyte conductivity measurement

All electrolyte conductivity was measured with the Traceable™ Conductivity Meter Pen (11714226, Fisher Scientific).

Standard nanoparticles characterization

The stability of the gold nanoparticles diluted in the KCl translocation buffer was probed by UV-Vis measurements using a NanoDrop ND-1000 spectrophotometer (Thermo Scientific). The size distribution and the Z potential of the standard nanoparticles in pure water and 20mM KCl solution was determined by Zetasizer NanoZS (Malvern Instruments Ltd.) and are shown in Fig S14 and S15. All the standard nanosphere samples were used as received.

Nanopore fabrication and characterization

The nanopores were fabricated starting from 1.0 mm x 0.5 mm quartz capillaries (QF120-90-10; Sutter Instrument, UK) with the SU-P2000 laser puller (World Precision Instruments, UK), using a two-line program: (1) HEAT, 750; FILAMENT, 4, VELOCITY, 30; DELAY, 145, PULL, 80; (2) HEAT, 600, FILAMENT, 3; VELOCITY, 40; DELAY, 135; PULL, 150. The pulling parameters



are instrument specific and lead to glass nanopore with a diameter of ≈ 60 nm. Adjustments of the HEAT AND PULL parameters were made to fabricate other pore sizes specified in this study. The pulled glass nanopores were characterized by measuring their pore resistance in 0.1 M KCl and the pore dimensions were confirmed by Scanning Electron Microscopy (SEM) using a Nova NanoSEM at an accelerating voltage of 3–5 kV.

View Article Online

DOI: 10.1039/D4FD00143E

Polymer electrolyte preparation

The KCl electrolyte was first dissolved with 18.2 M Ω ddH₂O to a final concentration of 1 M, the solution was then filtered through a 0.22 μ m syringe membrane filter (E4780-1223; Starlab UK). For example, to generate 10 ml of the 50% (w/v) PEG with 20 mM KCl, 0.2 ml of the 0.22 μ m filtered 1 M salt solution, 4.8 ml of 0.22 μ m filtered 18.2 M Ω ddH₂O and 5g of PEG 35 kDa (ultrapure grade, Sigma Aldrich) were mixed inside a tube. The tube was then left inside a 70°C incubator for 2 hours and then kept at 37°C overnight. The tubes were then left on bench for 4 hours to reach the room temperature prior use. The polymer electrolyte was then stored at room temperature.

Nanopore translocation measurements

An Ag/AgCl wire (0.25 mm diameter, GoodFellow UK) was inserted in the glass nanopore barrel and acted as the working electrode, while a second Ag/AgCl wire was immersed in the bath and acted as the counter and reference electrodes. In some experiments, a Ag/AgCl frit filled with 20mM KCl was used. The nanoparticles were driven from the external bath into the nanopipette by applying a positive potential to the working electrode placed inside the glass nanopore with respect to the reference electrode in the bath. The ion current was recorded either with a MultiClamp 700B patch-clamp amplifier (Molecular Devices) in voltage-clamp mode at a 100 kHz sampling rate with a 20 kHz low-pass filter



using the pClamp10 software (Molecular Devices) or using the Nanopore Reader (Elements srl) 100 kHz sampling rate with a 20 kHz low-pass filter.

View Article Online
DOI: 10.1039/D4FD00143E

Nanoimpact measurements

Nanoimpact electrochemistry experiments were performed using a 2-electrode configuration using a Pt microelectrode (10 μm in diameter) as working electrode and a Ag/AgCl frit filled with 20 mM KCl as reference/counter electrode. Data were acquired with the nanopore reader (Elements srl) with a 100 kHz sampling rate and a 20 kHz low-pass filter.

Numerical simulations

Numerical simulations describing the electric potential and ion concentrations within and around the glass nanopore filled with polymer electrolyte described as a truncated cone. The simulations were implemented using the commercial finite element software COMSOL Multiphysics (version 6.0 & Chemical Reaction Engineering module) to solve the couple Poisson Nernst-Planck equations (see SI). The simulations are based on our model of a glass nanopore immersed in a polymer electrolyte¹⁴ and are described briefly below. Further details, including determination of physical parameters, can be found in Supporting Information.

Boundary conditions, which are listed in the SI, were chosen to reflect the experimental system, and include an applied potential at the internal electrode vs an external electrode at ground, surface charge on, and no ion transport through, the glass walls, and bulk solution concentrations. Ion transport depends on the phase (PEG+KCl or KCl) with diffusion coefficients chosen to match the experimentally measured solution conductivities. In KCl, the diffusion coefficients of the K^+ and Cl^- are approximately equal¹⁷ ($D_{\text{K}^+}:D_{\text{Cl}^-} = 0.49:0.51$)



while in the PEG Cl⁻ is more mobile¹⁴ with the ratio $D_{K^+}:D_{Cl^-} = 0.45:0.55$ (see Supporting Information for details). For simplicity, we took the interface between the PEG+KCl and KCl to have zero width, i.e., mixing of the solutions was neglected, with the interface determined to reside inside the pipette by $\sim 8 \mu\text{m}$ (see Supporting Information for details).

View Article Online

DOI: 10.1039/D4FD00143E

DECLARATION OF INTERESTS

The authors declare no competing interests.

ACKNOWLEDGEMENTS

We thank Dr Alexander Kulak for the help provided with SEM imaging of the glass nanopores. S.C., K.T., P.A. acknowledge funding from the European Union's Horizon 2020 research and innovation 7 program under the Marie Skłodowska-Curie MSCA-ITN grant agreement no. 812398, through the single-entity nanoelectrochemistry, SENTINEL, project. P.A. Acknowledge funding from the European Research Council (ERC) under the project DYNAMIN, grant agreement no. 788968. P.A., C.C. and C.W. acknowledge funding from the Engineering and Physical Sciences Research Council UK (EPSRC) Healthcare Technologies for the grant EP/W004933/1, and S.C. and C.W. acknowledges funding from the Medical Research Council (MRC) UK under the grant number MR/N029976/1. Numerical simulations made use of resources available at the Arkansas High Performance Computing Center supported in part by National Science Foundation grants #0722625, #0959124, #0963249,



#0918970 and the Arkansas Science and Technology Authority. The work in the Edwards lab

View Article Online

DOI: 10.1039/D4FD00143E

was supported by the Arkansas Biosciences Institute.

DATA AVAILABILITY

The data that support the findings of this study are openly available from the University of Leeds data repository at <https://doi.org/TBD5>.

REFERENCES

1. N. Joudeh and D. Linke, Nanoparticle classification, physicochemical properties, characterization, and applications: a comprehensive review for biologists, *Journal of Nanobiotechnology*, 2022, **20**.
2. W. J. Stark, P. R. Stoessel, W. Wohlleben and A. Hafner, Industrial applications of nanoparticles, *Chemical Society Reviews*, 2015, **44**, 5793-5805.
3. M. M. Modena, B. Rühle, T. P. Burg and S. Wuttke, Nanoparticle Characterization: What to Measure?, *Advanced Materials*, 2019, **31**.
4. S. Gimondi, H. Ferreira, R. L. Reis and N. M. Neves, Microfluidic Devices: A Tool for Nanoparticle Synthesis and Performance Evaluation, *ACS Nano*, 2023, **17**, 14205-14228.
5. X. Xu, D. Valavanis, P. Ciocci, S. Confederat, F. Marcuccio, J.-F. Lemineur, P. Actis, F. Kanoufi and P. R. Unwin, The New Era of High-Throughput Nanoelectrochemistry, *Analytical Chemistry*, 2023, **95**, 319-356.
6. E. Tomaszewska, K. Soliwoda, K. Kadziola, B. Tkacz-Szczesna, G. Celichowski, M. Cichomski, W. Szmaja and J. Grobelny, Detection Limits of DLS and UV-Vis Spectroscopy in Characterization of Polydisperse Nanoparticles Colloids, *Journal of Nanomaterials*, 2013, **2013**, 1-10.



7. V. Filipe, A. Hawe and W. Jiskoot, Critical Evaluation of Nanoparticle Tracking Analysis (NTA) by NanoSight for the Measurement of Nanoparticles and Protein Aggregates, *Pharmaceutical Research*, 2010, **27**, 796-810.
8. L. Xue, H. Yamazaki, R. Ren, M. Wanunu, A. P. Ivanov and J. B. Ediel, Solid-state nanopore sensors, *Nature Reviews Materials*, 2020, **5**, 931-951.
9. S. R. German, L. Luo, H. S. White and T. L. Mega, Controlling Nanoparticle Dynamics in Conical Nanopores, *The Journal of Physical Chemistry C*, 2012, **117**, 703-711.
10. C. Chau, F. Marcuccio, D. Soulias, M. A. Edwards, A. Tuplin, S. E. Radford, E. Hewitt and P. Actis, Probing RNA Conformations Using a Polymer–Electrolyte Solid-State Nanopore, *ACS Nano*, 2022, **16**, 20075-20085.
11. C. C. Chau, S. E. Radford, E. W. Hewitt and P. Actis, Macromolecular Crowding Enhances the Detection of DNA and Proteins by a Solid-State Nanopore, *Nano Letters*, 2020, **20**, 5553-5561.
12. S. Confederat, I. Sandei, G. Mohanan, C. Walti and P. Actis, Nanopore fingerprinting of supramolecular DNA nanostructures, *Biophys J*, 2022, **121**, 4882-4891.
13. S. Confederat, S. Lee, D. Vang, D. Soulias, F. Marcuccio, T. I. Peace, M. A. Edwards, P. Strobba, D. Samanta, C. Wälti and P. Actis, Next-Generation Nanopore Sensors Based on Conductive Pulse Sensing for Enhanced Detection of Nanoparticles, *Small*, 2023, **20**.
14. F. Marcuccio, D. Soulias, C. C. C. Chau, S. E. Radford, E. Hewitt, P. Actis and M. A. Edwards, Mechanistic Study of the Conductance and Enhanced Single-Molecule Detection in a Polymer–Electrolyte Nanopore, *ACS Nanoscience Au*, 2023, **3**, 172-181.
15. M. Azimzadeh Sani and K. Tschulik, Unveiling colloidal nanoparticle properties and interactions at a single entity level, *Current Opinion in Electrochemistry*, 2023, **37**, 101195.
16. C. Wei, A. J. Bard and S. W. Feldberg, Current Rectification at Quartz Nanopipet Electrodes, *Analytical Chemistry*, 1997, **69**, 4627-4633.
17. W. M. Haynes, ed., *CRC Handbook of Chemistry and Physics*, Boca Raton, 2016.

View Article Online
DOI: 10.1039/D4FD00143E



18. W.-J. Lan, M. A. Edwards, L. Luo, R. T. Perera, X. Wu, C. R. Martin and H. S. White, Voltage-Rectified Current and Fluid Flow in Conical Nanopores, *Accounts of Chemical Research*, 2016, **49**, 2605-2613. View Article Online
DOI: 10.1039/C6CY00143E
19. R. R. de Oliveira, C. Avila, R. Bourne, F. Muller and A. de Juan, Data fusion strategies to combine sensor and multivariate model outputs for multivariate statistical process control, *Analytical and Bioanalytical Chemistry*, 2020, **412**, 2151-2163.
20. V. Shkirskiy and F. Kanoufi, Key requirements for advancing machine learning approaches in single entity electrochemistry, *Current Opinion in Electrochemistry*, 2024, **46**, 101526.
21. H. Chen, E. Kätelhön and R. G. Compton, Machine learning in fundamental electrochemistry: Recent advances and future opportunities, *Current Opinion in Electrochemistry*, 2023, **38**, 101214.
22. Z. Zhao, A. Naha, N. Kostopoulos and A. Sekretareva, Advanced Algorithm for Step Detection in Single-Entity Electrochemistry: A Comparative Study of Wavelet Transforms and Convolutional Neural Networks, *Faraday Discussions*, 2024, DOI: 10.1039/d4fd00130c.
23. P. Pandey, N. Bhattarai, L. Su, X. Wang, F. Leng, B. Gerstman, P. P. Chapagain and J. He, Detecting Individual Proteins and Their Surface Charge Variations in Solution by the Potentiometric Nanoimpact Method, *ACS Sensors*, 2022, **7**, 555-563.
24. P. Pandey, A. Sesena-Rubfiaro, S. Khatri and J. He, Development of multifunctional nanopipettes for controlled intracellular delivery and single-entity detection, *Faraday Discussions*, 2022, **233**, 315-335.
25. R. Ren, Y. Zhang, B. P. Nadappuram, B. Akpınar, D. Klenerman, A. P. Ivanov, J. B. Edl and Y. Korchev, Nanopore extended field-effect transistor for selective single-molecule biosensing, *Nature Communications*, 2017, **8**.
26. M. A. Edwards, S. R. German, J. E. Dick, A. J. Bard and H. S. White, High-Speed Multipass Coulter Counter with Ultrahigh Resolution, *ACS Nano*, 2015, **9**, 12274-12282.
27. T. Kawaguchi, M. Tsutsui, S. Murayama, I. W. Leong, K. Yokota, Y. Komoto and M. Taniguchi, Enhanced Nanoparticle Sensing in a Highly Viscous Nanopore, *Small Methods*, 2024, DOI: 10.1002/smt.202301523.



28. S. Liang, A. B. Kinghorn, M. Voliotis, J. K. Prague, J. D. Veldhuis, K. Tsaneva-Atanasova, C. A. McArdle, R. H. W. Li, A. E. G. Cass, W. S. Dhillon and J. A. Tanner, [View Article Online](#) DOI: 10.1039/D4FD00143E
Measuring luteinising hormone pulsatility with a robotic aptamer-enabled electrochemical reader, *Nature Communications*, 2019, **10**.
29. C. C. Chau, C. M. Maffeo, A. Aksimentiev, S. E. Radford, E. W. Hewitt and P. Actis, Single molecule delivery into living cells, *Nature Communications*, 2024, **15**.



The data that support the findings of this study are openly available from the University of Leeds data repository at <https://doi.org/TBD5>

View Article Online
DOI: 10.1039/D4FD00143E

Open Access Article. Published on 22 July 2024. Downloaded on 7/29/2024 12:31:07 PM.
This article is licensed under a Creative Commons Attribution 3.0 Unported Licence.

